

---

# Using Weight Mirrors to Improve Feedback Alignment

---

**Mohamed Akrouf**  
University of Toronto

**Collin Wilson**  
University of Toronto

**Peter C. Humphreys**  
DeepMind

**Timothy Lillicrap**  
DeepMind, University College London

**Douglas Tweed**  
University of Toronto, York University

## Abstract

Current algorithms for deep learning probably cannot run in the brain because they rely on *weight transport*, in which forward-path neurons transmit their synaptic weights to a feedback path, in a way that is likely impossible biologically. An algorithm called *feedback alignment* achieves deep learning without weight transport by using random feedback weights, but it performs poorly on hard visual-recognition tasks. Here we describe a neural circuit called a *weight mirror*, which lets the feedback path learn appropriate synaptic weights quickly and accurately even in large networks, without weight transport or complex wiring, and with a Hebbian learning rule. Tested on the ImageNet visual-recognition task, networks with weight mirrors outperform both plain feedback alignment and the newer sign-symmetry method, and nearly match the error-backpropagation algorithm, which uses weight transport.

## 1 Introduction

The algorithms of deep learning were devised to run on computers, yet in many ways they seem suitable for brains as well; for instance, they use multilayer networks of processing units, each with many inputs and a single output, like networks of neurons. But current algorithms can't quite work in the brain because they rely on *weight transport*: each unit multiplies its incoming signals by numbers called weights, and some units transmit their weights to other units. In the brain, it is the synapses that perform this weighting, but there is no known pathway by which they can transmit their weights to other neurons or to other synapses in the same neuron [1, 2].

Lillicrap et al. in [3] offered a solution in the form of *feedback alignment*, a mechanism that lets deep networks learn without weight transport, and they reported good results on several tasks. But Bartunov et al. [4] and Moskovitz et al. [5] have found that feedback alignment does not scale to hard visual recognition problems such as CIFAR-10 [6] and ImageNet [7].

Xiao et al. in [8] achieved good performance on ImageNet using a *sign-symmetry* algorithm in which only the signs of the forward and feedback weights, not necessarily their values, must correspond, and they suggested a mechanism by which that correspondence might be set up during brain development.

Here we propose a different approach that learns ImageNet almost as well as backprop does, with no need to initialize forward and feedback matrices so their signs agree. We describe a circuit called a *weight mirror*, which lets initially random feedback weights learn appropriate values without weight transport. These weights are trained layer-wise, and in this respect our mechanism resembles difference target propagation [4], which also shapes the feedback pathway layer by layer, but target propagation learns approximate layer-wise autoencoders (though see [9]), and uses feedback weights to propagate targets rather than gradients.

There are of course other questions about the biological implications of deep-learning algorithms, some of which we touch on later, in Section 8, but in this paper our main concern is with weight transport.

## 2 The weight-transport problem

In a typical deep-learning network, some signals flow along a *forward path* through multiple layers of processing units from the input layer to the output, while other signals flow back from the output layer along a *feedback path*. Forward-path signals perform inference (e.g. they try to infer what objects are depicted in a visual input) while the feedback path conveys error signals that guide learning. In the forward path, signals flow according to the equation:

$$\mathbf{y}_{l+1} = \phi(\mathbf{W}_{l+1} \mathbf{y}_l + \mathbf{b}_{l+1}) \quad (1)$$

Here  $\mathbf{y}_l$  is the output signal of layer  $l$ , i.e. a vector whose  $i$ -th element is the activity of unit  $i$  in layer  $l$ . Equation 1 shows how the next layer  $l + 1$  processes its input  $\mathbf{y}_l$ : it multiplies  $\mathbf{y}_l$  by the forward weight matrix  $\mathbf{W}_{l+1}$ , adds a bias vector  $\mathbf{b}_{l+1}$ , and puts the sum through an activation function  $\phi$ . Interpreted as parts of a real neuronal network in the brain, the  $\mathbf{y}$ 's might be vectors of neuronal firing rates, or some function of those rates,  $\mathbf{W}_{l+1}$  might be arrays of synaptic weights, and  $\mathbf{b}_{l+1}$  and  $\phi$  bias currents and nonlinearities in the neurons.

In the feedback path, error signals  $\delta$  flow through the network from its output layer according to the error-backpropagation [10] or *backprop* equation:

$$\delta_l = \phi'(\mathbf{y}_l) \mathbf{W}_{l+1}^T \delta_{l+1} \quad (2)$$

Here  $\phi'$  is the derivative of the activation function  $\phi$  from equation (1), which can be computed from  $\mathbf{y}_l$ . So feedback signals pass layer by layer through weights  $\mathbf{W}_l^T$ . Interpreted as a structure in the brain, we may think of the feedback path as another set of neurons, distinct from those in the forward path, or we may suppose that the same set of neurons carries inference signals in one direction and errors in the other [11, 12].

Either way, we have the problem that the same weight matrix  $\mathbf{W}_l$  appears in the forward equation (1) and then again, transposed, in the feedback equation (2), whereas in the brain, the synapses in the forward and feedback paths are physically distinct, with no known way to coordinate themselves so one set is always the transpose of the other [1, 2].

## 3 Feedback alignment

In feedback alignment, the problem is avoided by replacing the transposed  $\mathbf{W}_l$ 's in the feedback path by random, fixed (non-learning) weight matrices  $\mathbf{B}_l$ ,

$$\delta_l = \phi'(\mathbf{y}_l) \mathbf{B}_{l+1} \delta_{l+1} \quad (3)$$

These feedback signals  $\delta$  drive learning in the forward weights  $\mathbf{W}$  by the rule

$$\Delta \mathbf{W}_{l+1} = -\eta_W \delta_{l+1} \mathbf{y}_l^T \quad (4)$$

where  $\eta_W$  is a learning-rate factor. As shown in [3], equations (1), (3), and (4) together drive the forward matrices  $\mathbf{W}_l$  to become roughly proportional to transposes of the feedback matrices  $\mathbf{B}_l$ . That rough transposition makes equation (3) similar enough to the backprop equation (2) that the network can learn simple tasks as well as backprop does.

Can feedback alignment be augmented to handle harder tasks? One approach is to adjust the feedback weights  $\mathbf{B}_l$  as well as the forward weights  $\mathbf{W}_l$ , to improve their agreement. Here we show how that adjustment can be achieved quickly and accurately in large networks without weight transport.

## 4 Learning the transpose

The aim is to adjust an initially random matrix  $\mathbf{B}$  so it becomes proportional to the transpose of another matrix  $\mathbf{W}$  without weight transport, i.e. given only the input and output vectors  $\mathbf{x}$  and  $\mathbf{y} = \mathbf{W}^T \mathbf{x}$  (for this explanation, we neglect the activation function  $\phi$ ). We observe that

$E[\mathbf{x}\mathbf{y}^T] = E[\mathbf{x}\mathbf{x}^T\mathbf{W}^T] = E[\mathbf{x}\mathbf{x}^T]\mathbf{W}^T$ . In the simplest case, if the elements of  $\mathbf{x}$  are independent and zero-mean with equal variance,  $\sigma^2$ , it follows that  $E[\mathbf{x}\mathbf{y}^T] = \sigma^2\mathbf{W}^T$ . Therefore we can push  $\mathbf{B}$  steadily in the direction  $\sigma^2\mathbf{W}$  using this *transposing rule*,

$$\Delta\mathbf{B} = \eta_B \mathbf{x}\mathbf{y}^T \quad (5)$$

So  $\mathbf{B}$  integrates a signal that is proportional to  $\mathbf{W}^T$  on average. Over time,  $\mathbf{B}$  may grow large, but if we add a mechanism such as weight decay to keep  $\|\mathbf{B}\|$  small [13–15], then the initial, random values in  $\mathbf{B}$  shrink away, and  $\mathbf{B}$  converges to a scalar multiple of  $\mathbf{W}^T$  (see Appendix A for an account of this learning rule in terms of gradient descent).

## 5 Weight mirrors

Here we describe one way the learning rule (5) might be implemented in a neural network of the form shown in Figure 1. We propose that the network alternates between two modes: an *engaged mode*, where it receives sensory inputs and adjusts its forward weights to improve its inference, and a *mirror mode*, where its neurons discharge noisily and adjust the feedback weights so they mimic the forward ones. Biologically, these two modes may correspond to wakefulness and sleep, or simply to practicing a task and then setting it aside for a moment.

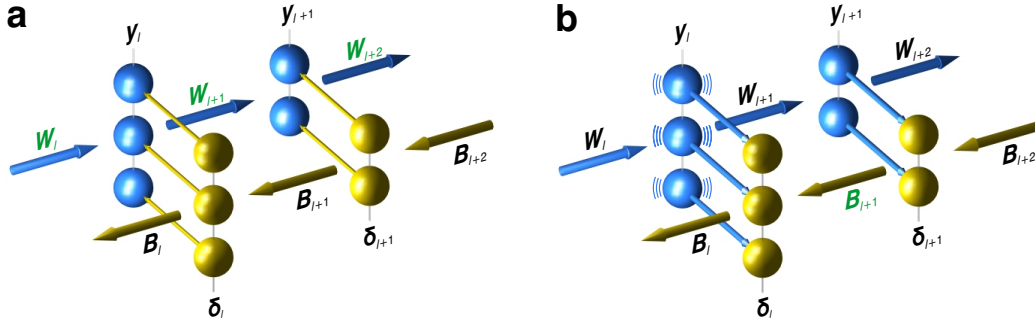


Figure 1: Network modes. Both panels show the same 2-layer section of a network. In both modes, the 3 neurons in layer  $l$  of the forward path (■) send their output signal  $y_l$  through the weight array  $\mathbf{W}_{l+1}$  (and other processing shown in equation (1)) to yield the next-layer signal  $y_{l+1}$ . And in the feedback path (■), the 2 neurons in layer  $l+1$  send their signal  $\delta_{l+1}$  through weight array  $\mathbf{B}_{l+1}$  to yield  $\delta_l$ , as in (3). The figure omits the biases  $\mathbf{b}$ , nonlinearities  $\phi$ , and, in the top panel, the projections that convey  $y_l$  to the  $\delta_l$  cells, allowing them to compute the factor  $\phi'(y_l)$  in equation (3). **a**) In *engaged mode*, cross-projections (■) convey the feedback signals  $\delta$  to the forward-path cells, so they can adjust the forward weights  $\mathbf{W}$  using learning rule (4). **b**) In *mirror mode*, one layer of forward cells, say layer  $l$ , fires noisily. Its signal  $y_l$  still passes through  $\mathbf{W}_{l+1}$  to yield  $y_{l+1}$ , but now the blue cross-projections control firing in the feedback path, so  $\delta_l = y_l$  and  $\delta_{l+1} = y_{l+1}$ , and the  $\delta_l$  neurons adjust the feedback weights  $\mathbf{B}_{l+1}$  using learning rule (7). We call the circuit  $y_l, y_{l+1}, \delta_{l+1}, \delta_l$  a *weight mirror* because it makes the weight array  $\mathbf{B}_{l+1}$  resemble  $\mathbf{W}_{l+1}^T$ .

The mirroring has two main elements: crosstalk and noise.

### 5.1 Crosstalk

In mirror mode, the forward-path neurons in each layer  $l$ , carrying the signal  $y_l$ , project strongly to layer  $l$  of the feedback path — strongly enough that each signal  $\delta_l$  of the feedback path faithfully mimics  $y_l$ , i.e.

$$\delta_l = y_l \quad (6)$$

### 5.2 Noise

In mirror mode, forward-path neurons fire noisily. Multiple layers may fire at once, but the process is simpler to explain in the case where they take turns, with just one layer  $l$  noisy at any one time. In that

case, all the cells of layer  $l$  fire randomly and independently, so their output signal  $\mathbf{y}_l$  has zero-mean and equal variance  $\sigma^2$ . That signal passes through forward weight matrix  $\mathbf{W}_{l+1}$  and activation function  $\phi$  to yield  $\mathbf{y}_{l+1} = \phi(\mathbf{W}_{l+1} \mathbf{y}_l + \mathbf{b}_{l+1})$ . By equation (6), signals  $\mathbf{y}_l$  and  $\mathbf{y}_{l+1}$  are transmitted to the feedback path. Then the layer- $l$  feedback cells adjust their weights  $\mathbf{B}_{l+1}$  by Hebbian learning,

$$\Delta \mathbf{B}_{l+1} = \eta_B \boldsymbol{\delta}_l \boldsymbol{\delta}_{l+1}^T \quad (7)$$

This circuitry and learning rule together constitute the weight mirror.

## 6 Why they work

To see that (7) approximates the transposing rule (5), notice first that

$$\boldsymbol{\delta}_l \boldsymbol{\delta}_{l+1}^T = \mathbf{y}_l \mathbf{y}_{l+1}^T = \mathbf{y}_l \phi(\mathbf{W}_{l+1} \mathbf{y}_l + \mathbf{b}_{l+1})^T \quad (8)$$

If we assume, for now, that  $\phi$  is everywhere differentiable, with derivatives everywhere positive, and if we make the variance  $\sigma^2$  of  $\mathbf{y}_l$  small enough that  $\mathbf{W}_{l+1} \mathbf{y}_l + \mathbf{b}_{l+1}$  falls in a roughly affine range of  $\phi$ , then

$$\phi(\mathbf{W}_{l+1} \mathbf{y}_l + \mathbf{b}_{l+1}) \approx \phi'(\mathbf{b}_{l+1}) (\mathbf{W}_{l+1} \mathbf{y}_l) + \phi(\mathbf{b}_{l+1}) \quad (9)$$

where  $\phi'(\mathbf{b}_{l+1})$  is a positive-definite, diagonal matrix. Therefore

$$\boldsymbol{\delta}_l \boldsymbol{\delta}_{l+1}^T \approx \mathbf{y}_l [\mathbf{y}_l^T \mathbf{W}_{l+1}^T \phi'(\mathbf{b}_{l+1})^T + \phi(\mathbf{b}_{l+1})^T] \quad (10)$$

and so

$$\begin{aligned} E[\Delta \mathbf{B}_{l+1}] &\approx \eta_B (E[\mathbf{y}_l \mathbf{y}_l^T] \mathbf{W}_{l+1}^T \phi'(\mathbf{b}_{l+1})^T + E[\mathbf{y}_l] \phi(\mathbf{b}_{l+1})^T) \\ &= \eta_B E[\mathbf{y}_l \mathbf{y}_l^T] \mathbf{W}_{l+1}^T \phi'(\mathbf{b}_{l+1})^T \\ &= \eta_B \sigma^2 \phi'(\mathbf{b}_{l+1}) \mathbf{W}_{l+1}^T \end{aligned} \quad (11)$$

Hence the weight matrix  $\mathbf{B}_{l+1}$  integrates a teaching signal (7) which is related to  $\mathbf{W}_{l+1}^T$  on average by a positive-definite, diagonal matrix  $\eta_B \sigma^2 \phi'(\mathbf{b}_{l+1})$ . Over time, this integration may drive up the matrix norm  $\|\mathbf{B}_{l+1}\|$ , but if we add a mechanism to keep the norm small — such as weight decay or synaptic scaling [14, 15] — then (7) makes  $\mathbf{B}_{l+1}$  approximately positive-definitely related to  $\mathbf{W}_{l+1}^T$ .

We can get a stronger result if we assume the biases  $\mathbf{b}_{l+1}$  are small, or if we suppose that neurons are capable of *bias-blocking* — of closing off their bias currents when in mirror mode, or preventing their influence on the axon hillock. Then

$$E[\Delta \mathbf{B}_{l+1}] \approx \eta_B \sigma^2 \phi'(\mathbf{0}) \mathbf{W}_{l+1}^T \quad (12)$$

So long as all neurons in forward layer  $l + 1$  have the same activation function, (12) implies that  $\mathbf{B}_{l+1}$  will come to approximate a positive *scalar* multiple of  $\mathbf{W}_{l+1}^T$ .

And with bias-blocking we can also drop the requirement that  $\phi$  have a positive derivative everywhere. Now it need only have a positive derivative near 0 (See Appendix 2 for a more general formulation that further relaxes the requirements on  $\phi$ ).

Next we will show that weight mirrors yield closer agreement between  $\mathbf{B}_{l+1}$  and  $\mathbf{W}_{l+1}^T$  than feedback alignment or sign symmetry do, and so enable better learning.

## 7 Experiments

We compared our mirroring algorithm to backprop, plain feedback alignment, and the sign-symmetry method [5, 8]. For easier comparison with recent papers on biologically-motivated algorithms [4, 5, 8], we used the same types of networks they did, with convolution [16], batch normalization (BatchNorm) [17], and rectified linear units (ReLU) without bias-blocking. In most experiments, we used a ResNet block variant where signals are normalized by BatchNorm after the ReLU nonlinearity, rather than before (see Appendix C.3). More brain-like implementations of the weight mirror would have to replace ReLU with a bounded function such as rectified tanh, convolution with non-weight-sharing local connections, and BatchNorm with some kind of synaptic scaling [14, 15].

Run on the ImageNet visual-recognition task [7] with the ResNet-18 network (Figure 2a), weight mirrors managed a final top-1 test error of 30.2(7)%, versus 97.4(2)% for plain feedback alignment, 39.2(4)% for sign-symmetry, and 30.1(4)% for backprop. With ResNet-50 (Figure 2b), the scores were: weight mirrors 23.4(5)%, feedback alignment 98.9(1)%, sign-symmetry 33.8(3)%, and backprop 22.9(4)%. (Digits in parentheses are standard uncertainties).

Sign-symmetry did better in other experiments (not shown) where batch normalization was applied *before* the ReLU nonlinearity. In those runs, it achieved top-1 test errors of 37.8(4)% with ResNet-18 (close to the 37.91% reported in [8] for the same network) and 32.6(6)% with ResNet-50 (see Appendix C.1 for details of our hyperparameter selection). The same change in BatchNorm made little difference to the other 3 methods — backprop, feedback alignment, and the weight mirror.

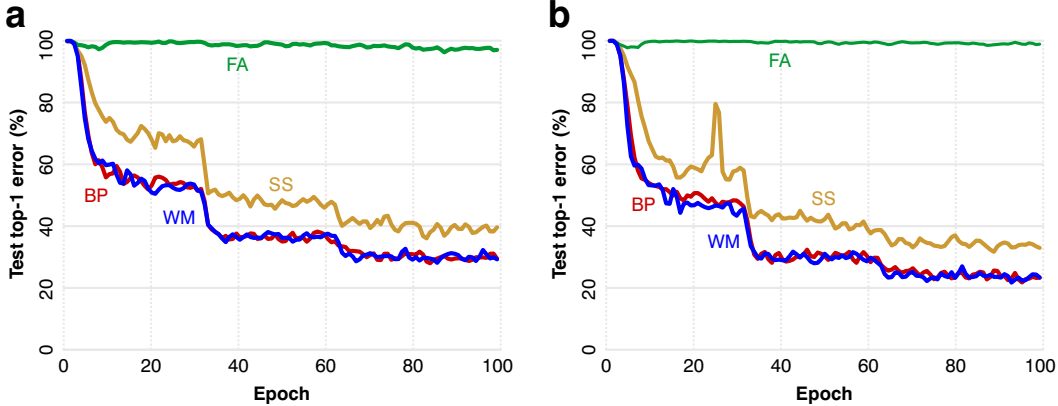


Figure 2: ImageNet results. **a)** With ResNet-18 architecture, the weight-mirror network (— WM) outperformed plain feedback alignment (— FA) and the sign-symmetry algorithm (— SS), and nearly matched backprop (— BP). **b)** With the larger ResNet-50 architecture, results were similar.

Weight mirroring kept the forward and feedback matrices in agreement throughout training, as shown in Figure 3. One way to measure this agreement is by matrix angles: in each layer of the networks, we took the feedback matrix  $\mathbf{B}_l$  and the transpose of the forward matrix,  $\mathbf{W}_l^T$ , and reshaped them into vectors. With backprop, the angle between those vectors was of course always 0. With weight mirrors (Figure 3a), the angle stayed  $< 12^\circ$  in all layers, and  $< 6^\circ$  later in the run for all layers except the final one. That final layer was fully connected, and therefore its  $\mathbf{W}_l$  received more inputs than those of the other, convolutional layers, making its  $\mathbf{W}_l^T$  harder to deduce. For closer alignment, we would have needed longer mirroring with more examples.

The matrix angles grew between epochs 2 and 10 and then held steady at relatively high levels till epoch 32 because during this period the learning rate  $\eta_W$  was large (see Appendix C.1), and mirroring didn't keep the  $\mathbf{B}_l$ 's matched to the fast-changing  $\mathbf{W}_l^T$ 's. That problem could also have been solved with more mirroring, but it did no harm because at epoch 32,  $\eta_W$  shrank by 90%, and from then on, the  $\mathbf{B}_l$ 's and  $\mathbf{W}_l^T$ 's stayed better aligned.

We also computed the  $\delta$  angles between the feedback vectors  $\delta_l$  computed by backprop (using  $\mathbf{W}_l^T$ 's) and those computed by the weight-mirror network (using  $\mathbf{B}_l$ 's). These angles stayed  $< 25^\circ$  in all layers (Figure 3b), with worse alignment farther upstream, because  $\delta$  angles depend on the accumulated small discrepancies between all the  $\mathbf{B}_l$ 's and  $\mathbf{W}_l^T$ 's in all downstream layers. By these same measures, the sign-symmetry method aligned matrices and  $\delta$ 's less accurately (Figures 3c and 3d). With feedback alignment (not shown), matrix and  $\delta$  angles stayed  $> 80^\circ$  for most layers in both the ResNet-18 and ResNet-50 architectures.

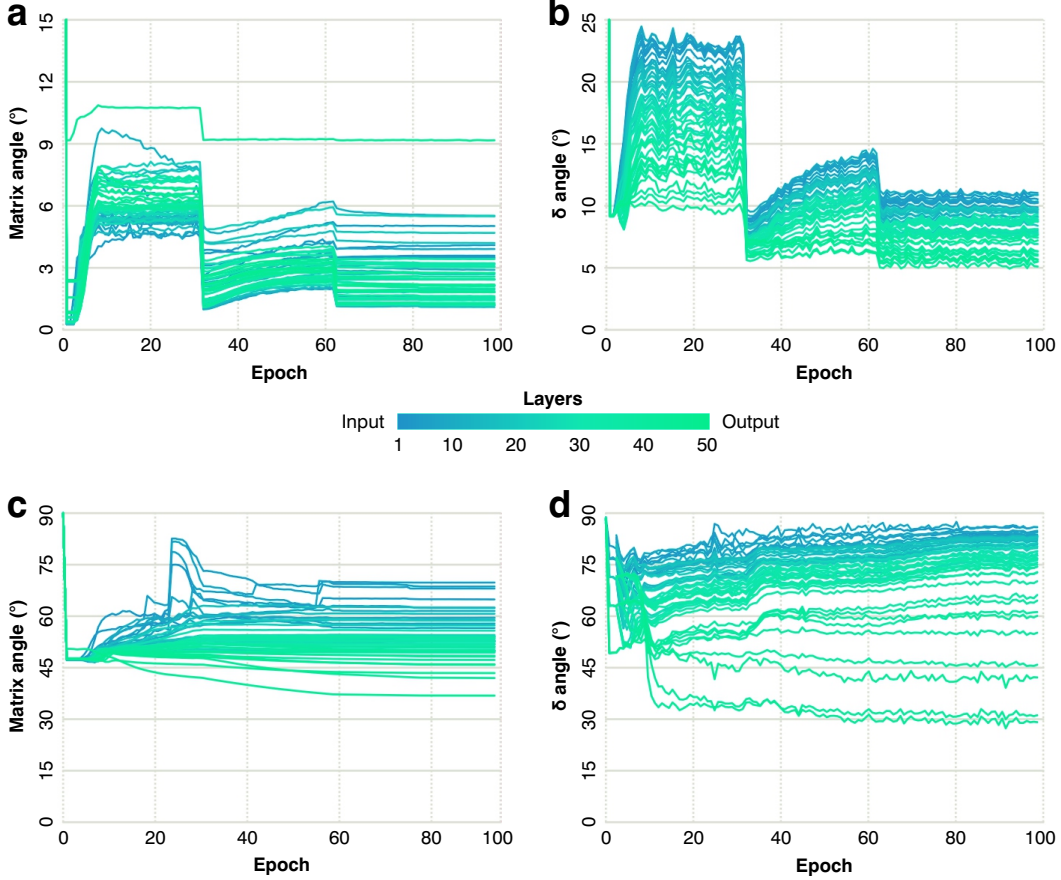


Figure 3: Agreement of forward and feedback matrices in the ResNet-50 from Figure 2b. **a)** Weight mirrors kept the angles between the matrices  $\mathbf{B}_l$  and  $\mathbf{W}_l^T$  small in all layers, from the input layer (—) to the output (—). **b)** Feedback vectors  $\delta_l$  computed by the weight-mirror network were also well aligned with those computed by backprop. **c, d)** The sign-symmetry method aligned matrices and  $\delta$ 's less accurately.

## 8 Biological interpretations

Our equations (1) and (3)–(7) can be interpreted physically in several different ways. Here we describe some issues and options:

### 8.1 Distinct feedback neurons?

Figure 1 shows a learning network where inference signals  $\mathbf{y}$  and error signals  $\delta$  are carried by distinct sets of neurons. But the equations work just as well if the same neurons carry inference signals in one direction and errors in the other. In some ways, that arrangement is simpler, because it needs no cross-projecting axons connecting two sets of cells. On the other hand, it faces greater challenges of signal segregation: how can  $\mathbf{y}$  and  $\delta$  flow through the same cells without interfering? Probably there are several solutions — e.g. neurons may segregate  $\mathbf{y}$  and  $\delta$  in different parts of the cell [18], or by multiplexing [19], or cells may take turns carrying one or the other signal — but the actual mechanisms and architectures used in the brain are open questions.

### 8.2 Zero-mean signals

In equation (11), we provided a rationale for our learning rule (7), but to do it we had to assume that the signal  $y_l$  had a zero mean. That assumption is awkward if we interpret the signals in our equations as firing rates of neurons, because neurons can't have negative rates, and so can't have zero

means except by remaining utterly silent. But we can drop the zero-mean requirement if we suppose that neurons convey positive and negative values by modulating about a baseline rate  $\beta$ . For instance, we might have

$$\mathbf{y}_{l+1} = \phi(\mathbf{W}_{l+1}(\mathbf{y}_l - \beta) + \mathbf{b}_{l+1}) \quad (13)$$

where  $\phi$  is a non-negative activation function and  $\mathbf{y}_l - \beta$  means that the same scalar  $\beta$  is subtracted from each element of the signal vector  $\mathbf{y}_l$ . In engaged mode, forward matrices are adjusted by the learning rule

$$\Delta \mathbf{W}_{l+1} = -\eta_W \delta_{l+1}(\mathbf{y}_l - \beta)^T \quad (14)$$

whereas in mirror mode,  $\mathbf{y}_l$  fires noisily with a mean of  $\beta$  rather than 0, and  $\mathbf{B}_{l+1}$  is adjusted by the rule

$$\Delta \mathbf{B}_{l+1} = \eta_B (\delta_l - \beta)(\delta_{l+1} - \beta)^T \quad (15)$$

This baseline parameter  $\beta$  may be built into forward and feedback neurons by the genome, or it may be estimated locally, for example by taking the average of the firing rates over a period of mirroring, as we did in our experiments. Another way to get positive and negative signals in the brain is to think of each processing unit not as a single neuron but as a group of cells acting in push-pull, some carrying positive signals and others negative [20]. Both mechanisms — baselines and push-pull — operate in the brain, for instance in the vestibulo-ocular reflex [21].

### 8.3 Cross-projections

If distinct neurons carry signals  $\mathbf{y}$  and  $\delta$  then the cross-projections between the forward and feedback paths must be axons, while if a single set of cells carries both  $\mathbf{y}$  and  $\delta$  then the cross-projections reflect some sort of intracellular signaling.

### 8.4 Multipurpose projections?

To avoid clutter, Figure 1a omitted the cross-projections which convey  $\mathbf{y}_l$  to the feedback cells, allowing them to compute the factor  $\phi'(\mathbf{y}_l)$  in equation (3). Figure 1b does show cross-projections from forward to feedback cells, carrying the same signal,  $\mathbf{y}_l$ , but having a different effect on the target cells, setting  $\delta_l = \mathbf{y}_l$ . We may interpret these two sets of projections — the ones omitted from Figure 1a and the ones drawn as thin blue arrows in 1b — as two distinct sets of axons carrying the same signal, or as a single set of axons whose effects on their targets differ in the two modes. Maybe these axons form two types of synapses, some onto ionotropic receptors and some onto metabotropic, or maybe some switch in intracellular signaling within the feedback cells makes them respond differently to identical signals.

### 8.5 Multilayer mirroring

In Figure 1b and accompanying text, we assumed that just one forward layer  $\mathbf{y}_l$  was noisy, and just one feedback array  $\mathbf{B}_{l+1}$  was adjusted, at any one time. Why not adjust all the  $\mathbf{B}$ 's at once? The problem is, when we adjust  $\mathbf{B}_{l+1}$  we need a zero-mean (or  $\beta$ -mean), uncorrelated, equal-variance signal  $\mathbf{y}_l$ , which drives  $\mathbf{y}_{l+1}$ . But the resulting  $\mathbf{y}_{l+1}$  generally will not be zero-mean, uncorrelated, or equal-variance, and so may not be effective at driving  $\mathbf{B}_{l+2}$  toward  $\mathbf{W}_{l+2}^T$ . We can of course apply noise simultaneously to every *second* layer — for instance to  $\mathbf{y}_2, \mathbf{y}_4, \mathbf{y}_6$ , etc. — and adjust as many as half the  $\mathbf{B}$ 's at any one moment, so the mirroring does not really have to proceed one layer at a time. And there may be other options in networks with batch normalization or synaptic scaling [17]. Those mechanisms tend to keep all the forward signals approximately zero-mean and equal-variance (though not uncorrelated), and in that case it may be possible to adjust all the  $\mathbf{B}$ 's at once, driving the entire network with a single noisy input vector  $\mathbf{y}_l$ , though we haven't tested that idea here.

## 9 Non-biological applications

The brain is not the only computing device that lacks weight transport. Abstractly, the issue is that the brain represents information in two different forms: some is coded in action potentials, which are energetically expensive but rapidly transmissible to other parts of the brain, while other information is stored in synaptic weights, which are cheap and compact but localized — they influence the transmissible signals but are not themselves transmitted. Similar issues arise in certain kinds of

technology, such as application-specific integrated circuits (ASICs). Here as in the brain, a mechanism like weight mirroring could allow forward and backward weights to live locally where they are used to compute activities. By transmitting only activities and not weights, such circuits might save time and energy [22–24].

## References

- [1] Stephen Grossberg. Competitive learning: From interactive activation to adaptive resonance. *Cognitive Science*, 11(1):23–63, 1987.
- [2] Francis Crick. The recent excitement about neural networks. *Nature*, 337(6203):129–132, 1989.
- [3] Timothy P Lillicrap, Daniel Cownden, Douglas B Tweed, and Colin J Akerman. Random synaptic feedback weights support error backpropagation for deep learning. *Nature Communications*, 7:13276, 2016.
- [4] Sergey Bartunov, Adam Santoro, Blake Richards, Luke Marris, Geoffrey E Hinton, and Timothy Lillicrap. Assessing the scalability of biologically-motivated deep learning algorithms and architectures. In *Advances in Neural Information Processing Systems*, pages 9390–9400, 2018.
- [5] Theodore H Moskovitz, Ashok Litwin-Kumar, and LF Abbott. Feedback alignment in deep convolutional networks. *arXiv preprint arXiv:1812.06488*, 2018.
- [6] Alex Krizhevsky and Geoffrey Hinton. Learning multiple layers of features from tiny images. Technical report, Citeseer, 2009.
- [7] Olga Russakovsky, Jia Deng, Hao Su, Jonathan Krause, Sanjeev Satheesh, Sean Ma, Zhiheng Huang, Andrej Karpathy, Aditya Khosla, Michael Bernstein, et al. Imagenet large scale visual recognition challenge. *International Journal of Computer Vision*, 115(3):211–252, 2015.
- [8] Will Xiao, Honglin Chen, Qianli Liao, and Tomaso Poggio. Biologically-plausible learning algorithms can scale to large datasets. *arXiv preprint arXiv:1811.03567*, 2018.
- [9] Daniel Kunin, Jonathan M Bloom, Aleksandrina Goeva, and Cotton Seed. Loss landscapes of regularized linear autoencoders. *arXiv preprint arXiv:1901.08168*, 2019.
- [10] David E Rumelhart, Geoffrey E Hinton, Ronald J Williams, et al. Learning representations by back-propagating errors. *Nature*, 323:533–536, 1986.
- [11] Robert Urbanczik and Walter Senn. Learning by the dendritic prediction of somatic spiking. *Neuron*, 81(3):521–528, 2014.
- [12] Jordan Guerguiev, Timothy P Lillicrap, and Blake A Richards. Biologically feasible deep learning with segregated dendrites. *arXiv preprint arXiv:1610.00161*, 2016.
- [13] Nathan Intrator and Leon N Cooper. Objective function formulation of the bcm theory of visual cortical plasticity: Statistical connections, stability conditions. *Neural Networks*, 5(1):3–17, 1992.
- [14] Gina G Turrigiano. The self-tuning neuron: synaptic scaling of excitatory synapses. *Cell*, 135(3):422–435, 2008.
- [15] Dhruvajyoti Chowdhury and Johannes W Hell. Homeostatic synaptic scaling: Molecular regulators of synaptic AMPA-type glutamate receptors. *F1000Research*, 7, 2018.
- [16] Yann LeCun, Bernhard Boser, John S Denker, Donnie Henderson, Richard E Howard, Wayne Hubbard, and Lawrence D Jackel. Backpropagation applied to handwritten zip code recognition. *Neural Computation*, 1(4):541–551, 1989.
- [17] Sergey Ioffe and Christian Szegedy. Batch normalization: Accelerating deep network training by reducing internal covariate shift. *arXiv preprint arXiv:1502.03167*, 2015.
- [18] Jordan Guerguiev, Timothy P Lillicrap, and Blake A Richards. Towards deep learning with segregated dendrites. *Elife*, 6:e22901, 2017.
- [19] Richard Naud and Henning Sprekeler. Sparse bursts optimize information transmission in a multiplexed neural code. *Proceedings of the National Academy of Sciences*, 115(27):E6329–E6338, 2018.
- [20] Chris Eliasmith and Charles H Anderson. *Neural engineering: Computation, representation, and dynamics in neurobiological systems*. MIT Press, 2004.



- [21] R.j Leigh and D.S. Zee. *The Neurology of Eye Movements*. New York: Oxford University Press, 3rd ed. edition, 1999.
- [22] Yu-Hsin Chen, Joel Emer, and Vivienne Sze. Eyeriss: A spatial architecture for energy-efficient dataflow for convolutional neural networks. In *ACM SIGARCH Computer Architecture News*, volume 44, pages 367–379. IEEE Press, 2016.
- [23] Hyoukjun Kwon, Michael Pellauer, and Tushar Krishna. Maestro: An open-source infrastructure for modeling dataflows within deep learning accelerators. *arXiv preprint arXiv:1805.02566*, 2018.
- [24] Brian Crafton, Abhinav Parihar, Evan Gebhardt, and Arijit Raychowdhury. Direct feedback alignment with sparse connections for local learning. *arXiv preprint arXiv:1903.02083*, 2019.
- [25] Kaiming He, Xiangyu Zhang, Shaoqing Ren, and Jian Sun. Deep residual learning for image recognition. In *Proceedings of the IEEE Conference on Computer Vision and Pattern Recognition*, pages 770–778, 2016.
- [26] Ilya Sutskever, James Martens, George E Dahl, and Geoffrey E Hinton. On the importance of initialization and momentum in deep learning. *ICML (3)*, 28(1139-1147):5, 2013.
- [27] Peter Buchlovsky, David Budden, Dominik Grewe, Chris Jones, John Aslanides, Frederic Besse, Andy Brock, Aidan Clark, Sergio Gómez Colmenarejo, Aedan Pope, et al. Tf-replicator: Distributed machine learning for researchers. *arXiv preprint arXiv:1902.00465*, 2019.

## Appendices

### A The transposing rule as gradient descent

The learning rule (5) can be expressed as a form of gradient descent,

$$\Delta \mathbf{B} = \eta \mathbf{x} \mathbf{y}^T = -\eta \frac{\partial f}{\partial \mathbf{B}} \quad (16)$$

where

$$f(\mathbf{x}, \mathbf{y}, \mathbf{B}) = -\text{sum}(\mathbf{x} \mathbf{y}^T \odot \mathbf{B}) = -\sum_{i,j} x^i y_j B_j^i \quad (17)$$

This function  $f$  is not a *loss* or *objective* function, as it has no minimum for any fixed, non-zero  $\mathbf{x}$  and  $\mathbf{y}$ , and neither is it a quantity we would *wish* to minimize, because it can be pushed farther and farther below zero by making  $\mathbf{B}$  larger and larger. But if we combine (5) with weight decay

$$\Delta \mathbf{B} = \eta_B \mathbf{x} \mathbf{y}^T - \lambda \mathbf{B} \quad (18)$$

then we do descend the gradient of a loss

$$\mathcal{L} = f + \frac{\lambda}{2\eta_B} \|\mathbf{B}\|^2 \quad (19)$$

### B Admissible activation functions

When we first described the weight mirror we assumed an activation function that dropped below zero in places (to allow zero-mean signals) and had a positive derivative everywhere, and then later we relaxed those requirements. Here we show that a generalization of bias-blocking and equations (13)–(15) lets us work with any activation function  $\phi$  so long there is some neighborhood where it is positive and has a positive derivative. We choose a *default bias*  $b^-$  inside that neighborhood, we define  $\beta = \phi(b^-)$ , and we make

$$\mathbf{y}_{l+1} = \phi(\mathbf{W}_{l+1}(\mathbf{y}_l - \beta) + \mathbf{b}_{l+1} + b^-) \quad (20)$$

In mirror mode, as before,  $\mathbf{y}_l$  has a mean of  $\beta$ ,  $\mathbf{b}_{l+1} = \mathbf{0}$ , and the learning rule is (15), so

$$\begin{aligned} \Delta \mathbf{B}_{l+1} &= \eta_B (\boldsymbol{\delta}_l - \beta) (\boldsymbol{\delta}_{l+1} - \beta)^T \\ &= \eta_B (\mathbf{y}_l - \beta) (\phi(\mathbf{W}_{l+1}(\mathbf{y}_l - \beta) + b^-) - \beta)^T \\ &\approx \eta_B (\mathbf{y}_l - \beta) (\phi'(b^-) \mathbf{W}_{l+1}(\mathbf{y}_l - \beta) + \phi(b^-) - \beta)^T \\ &= \eta_B (\mathbf{y}_l - \beta) (\mathbf{y}_l - \beta)^T \phi'(b^-) \mathbf{W}_{l+1}^T \end{aligned} \quad (21)$$

which means  $\mathbf{B}_{l+1}$  is again driven to a positive scalar multiple of  $\mathbf{W}_{l+1}^T$ .

## C Experimental details

### C.1 Architecture and training

Experiments were carried out using 18- and 50-layer deep-residual networks ResNet-18 and ResNet-50 [25]. Their architecture consists of a sequence of sub-blocks, each made up of two (ResNet-18) or three (ResNet-50) convolutional layers in series. In parallel with these layers is a shortcut connection whose output is added to the output from the convolutional layers. In [25], each convolutional layer is followed by batch normalization and then a ReLU nonlinearity, but in most of our experiments, we applied batch normalization *after* the ReLU function. The output of the network passed through a final fully-connected layer followed by a softmax.

For the sign-symmetry algorithm, we carried out grid searches of the learning rate over the range [0.01, 2.0] while running training out to 140 epochs to ensure convergence. We found that 0.5 gave the lowest top-1 errors with both ResNet-18 and ResNet-50, and so we used that value for all

sign-symmetry experiments. Otherwise, all hyperparameters in all algorithms (except those for mirror mode) were taken from [20], including forward-path Nesterov momentum [26] 0.9 and weight decay (L2 regularizer)  $10^{-4}$ . We used TF-Replicator [27] to distribute training across 32 workers, for a total mini-batch of 2048 images. And we applied the annealing schedule from [27], i.e.  $\eta_W$  grew linearly over the first 6 epochs (or over epochs 3 to 8 for weight-mirror networks, see below), and shrank 10-fold after epochs 32, 62, and 82.

## C.2 Mirroring

Each weight-mirror network spent its first 2 epochs entirely in mirror mode, bringing its initial, random weights into alignment. Thereafter, it did a small amount of mirroring after each mini-batch of engaged-mode learning. It mirrored layer-wise: it created a new mini-batch of noisy activity in layer  $l$  (independent Gaussian signals with zero mean and unit variance across the 2048 examples in the mirroring mini-batch) and it sent those signals through the convolutional layer and then the ReLU function. It computed the means of the post-ReLU outputs across the mini-batch and subtracted them to give zero-mean outputs in each layer.

As in equation (18), the covariance matrix of these zero-mean signals was estimated by multiplying them and averaging over the mini-batch. In convolutional layers, because of weight sharing, each weight connected multiple sets of inputs and outputs, and so we estimated the covariance associated with any given weight by averaging the estimated covariances over the pairs of inputs and outputs it connected.

We used these covariance estimates to train the feedback weights, as in (18), with a learning-rate factor  $\eta_B$  of 0.1 and a weight decay  $\lambda$  of 0.5.

## C.3 Batch normalization

The weight mirror learned to match feedback matrices  $\mathbf{B}_l$  to forward matrices  $\mathbf{W}_l$ , but it did not try to mirror the batch normalization parameter vectors  $\boldsymbol{\mu}$  or  $\boldsymbol{\sigma}$  used in the forward path. In fact no  $\mathbf{B}_l$  could have mirrored the combined effects of  $\mathbf{W}_l$ ,  $\boldsymbol{\mu}$ , and  $\boldsymbol{\sigma}$  in our convolutional networks, because the  $\mathbf{B}_l$  matrices had the same convolutional, weight-sharing structure as the  $\mathbf{W}_l$ 's did — a structure which  $\boldsymbol{\mu}$  and  $\boldsymbol{\sigma}$  ignored. Therefore we simply passed the scaling parameter  $\boldsymbol{\sigma}$  from the forward to the feedback path ( $\boldsymbol{\mu}$  was not needed). This transfer involved very little information — just one scalar variable per feedback neuron. And it could be avoided if we replaced convolution by more biological local connections *without* weight sharing, as then the mirror *would* be able to learn normalization parameters.